# Effects of Resonant Magnetic Fluctuations on Plasma Confinement in Current Carrying high-$\beta$ Plasmas of LHD

Satoru SAKAKIBARA, Kiyomasa WATANABE, Hiroshi YAMADA, Yoshiro NARUSHIMA, Kazuo TOI, Satoshi OHDACHI, Taiki YAMAGUCHI[1)], Kazumichi NARIHARA, Kenji TANAKA, Tokihiko TOKUZAWA, Katsumi IDA, Osamu KANEKO, Kazuo KAWAHATA and Akio KOMORI and LHD Experimental Group

*National Institute for Fusion Science, Toki 509-5292, Japan*

[1)] *Department of Fusion Science, Graduate University for Advanced Studies, Toki 509-5292, Japan*

(Received 1 August 2005 / Accepted 9 December 2005)

The effects of resonant magnetic fluctuations on plasma confinement have been investigated in current carrying high-$\beta$ plasmas in magnetic hill configurations of the Large Helical Device. The $m/n$= 2/1 mode excited in core region was dominantly observed in the unstable configuration as predicted by linear theory on ideal instability, and the plasma current decreasing magnetic shear enhances the mode activity. The disappearance of the $m/n = 2/1$ mode was observed with an increase in plasma current, and then the plasma confinement and the beta value increase by less than 10 % with the recovery of core pressure. When the plasma current exceeds a certain value, the plasma confinement is improved by 20 % with the reduction of the amplitudes of the modes in the peripheral region in addition to the disappearance of the $m/n = 2/1$ mode. Then the beta value increases by 38 %. MHD activities led to no disruption even in such an *unstable* configuration, and the moderate plasma current mitigated the effect of MHD activity on the plasma confinement.

© *2006 The Japan Society of Plasma Science and Nuclear Fusion Research*

Keywords: MHD, interchange mode, heliotron, magnetic fluctuation, high-beta

DOI: 10.1585/pfr.1.003

## 1. Introduction

An understanding of MHD instability, which may lead to a $\beta$–limit, is a major subject for realization of an efficient fusion reactor with magnetic confinement system. $\beta$–limits due to resistive wall mode [1] and neoclassical tearing mode [2] have been observed in various tokamak experiments, and real-time control for their stabilization has been experimentally investigated. In helical plasmas, stabilization of pressure-driven modes such as ideal and/or resistive interchange modes is an essential issue for a production of high-$\beta$ plasma because the net toroidal current is small enough to excite current-driven instabilities. While a clear limitation of the beta value due to instabilities such as disruptive phenomena has not been found in the standard operation of any helical device, the variation of plasma profiles with resonant magnetic fluctuations [3] and minor collapse caused by formation of a steep pressure gradient in the vicinity of the resonant surface after pellet injection [4] have been observed in the core plasmas of the Large Helical Device (LHD). These phenomena have been well observed in marginal regions against the ideal interchange mode [5]. On the other hand, amplitudes of resonant fluctuations in peripheral region with magnetic hill are enhanced with increases in the beta value and the pressure gradient [6], and effects of their modes on global energy confinement have been observed in the high-$\beta$ region [7].

Characteristics of MHD modes strongly depend on the magnetic configuration as well as plasma parameters such as beta value, plasma profiles and so on. In particular, positive plasma current increasing the rotational transform leads to a decrease in the magnetic shear and the suppression of the Shafranov shift, which restrains the formation of a magnetic well. The positive current also affects the existence of the resonant surfaces. In ohmic heating experiments of the Compact Helical System (CHS), the excitation and the disappearance of different resonant fluctuations occur one after another with an increase in positive plasma current, and rapid changes of plasma confinement have been observed just after the disappearance of the resonant surface [8,9]. This suggests that these kinds of experiments enable us to clarify the relationship between the plasma confinement and the resonant fluctuations, and they also contribute to an understanding of the significance of magnetic shear from the viewpoint of MHD instability.

This article presents the effects of resonant magnetic fluctuations on plasma confinements in high-$\beta$ plasmas with finite plasma currents of LHD. The net plasma currents are induced primarily by beam driven currents and bootstrap currents [10]. The selected magnetic configuration is most unfavorable in term of the ideal interchange instability in the present operational regime. Therefore, it

*author's e-mail: sakakis@lhd.nifs.ac.jp*



© 2006 The Japan Society of Plasma Science and Nuclear Fusion Research

is favorable within the scope of the validity of theoretical prediction of linear MHD theory. The main focusing points are the changes in characteristics of plasmas with/without resonant magnetic fluctuations. In Sec. 2, the magnetic configuration and the measurement system in LHD are described. Typical discharges with different plasma currents and the appearance regime of resonant fluctuations are given in Sec. 3.1 and 3.2, respectively. The characteristics of plasma parameters before and after the disappearance of resonant fluctuations are described in Sec. 3.3. A discussion and summary are given in Sec. 4.

## 2. Experimental Setup

The LHD is the largest superconducting heliotron-type device. A confinement magnetic field is produced by $l$= 2/$N$= 10 continuous helical coils and three pairs of poloidal coils, where $l$ and $N$ are the poloidal and the toroidal mode number of the helical coil, respectively [11]. The major radius $R$ is 3.9 m and the averaged minor radius $a$ is 0.5 ~ 0.65 m. The magnetic configuration is characterized by a magnetic axis position, $R_{ax}$, which can be widely set by controlling poloidal coil currents from 3.5 to 4.1 m. The outward-shifted plasma is favorable for MHD stability because of magnetic well formation, while the inward-shifted plasma has an advantage in neoclassical transport and particle confinement because of its good particle orbit. Here the most inward-shifted configuration is selected for investigating the effects of MHD activity on the plasma confinement.

There are three tangential neutral beam injection (NBI) systems, and the directions of their injections can be turned over by changing the polarities of the poloidal and helical coils. Usually, two co- NBI's and one counter-NBI are applied.

For identification of the mode structure, 16 and 6 three-axial magnetic probes have been used as helical and toroidal arrays, respectively. The sampling frequency was 100 kHz, and signals were digitized through a low-pass filter of 50 kHz in the time range from 0.4 s to 3.0 s. Coherent modes with $m \leq 3$ and $n \leq 4$ were identified, where $m$ and $n$ are poloidal and toroidal mode numbers, respectively. The identification of the $m$ number using helical probe array was relatively difficult compared with that of the $n$ number because magnetic surfaces with an elliptical shape rotate toroidally in addition to the toroidal effect. Therefore the $m$ number was identified through a comparison between the spatial structure measured with a helical array and that calculated by multi-filament currents with the specific Fourier mode flowing onto the resonant surface. The locations of resonant surfaces were estimated by three-dimensional MHD equilibrium code VMEC [12] and their filaments were put on Boozer coordinates.

The volume averaged beta value, $\langle\beta_{dia}\rangle$, is defined as $\langle\beta_{dia}\rangle = (4\mu_0/3)W_p/(V_{p0}B_{av0}^2)$, where $W_p$ is the stored energy estimated by the diamagnetic flux measurement. $V_{p0}$ and $B_{av0}$ are the plasma volume and toroidal field averaged inside the last closed flux surface, respectively, and they are decided in vacuum configuration. The plasma current was measured with Rogowski coils inside vacuum vessel. The electron temperature profile was measured with a multi-point (200) and repetitive (50~200 kHz) Thomson scattering system. The spatial and time resolutions were 0.025 m and 0.02 s, respectively. A multi-channel FIR interferometer was used for measurement of electron density profile.

## 3. Experimental Results

Experiments were performed in configurations of $R_{ax}$ = 3.5 m and $B_t$ = 0.5 T, where $B_t$ is a toroidal magnetic field at $R_{ax}$. Operations with different polarities of $B_t$ were performed here for controlling the plasma currents composed of Ohkawa currents and bootstrap currents, and they make the productions of co- or counter dominant plasmas possible.

### 3.1 MHD activities in the small current plasmas

Figure 1 shows MHD activities in a high-$\beta$ discharge with small plasma currents. Two counter beams and one co- beam were injected from 0.3 s for the production of the target plasma and could maintain it to 1.86 s as shown in Fig.1(a). The total absorption power of neutral beams, $P_{abs}$, approached about 6.5 MW at 1.33 s. The temporal changes of $\langle\beta_{dia}\rangle$ and line averaged electron density, $\bar{n}_e$ are shown in Fig.1(b). The electron density is fueled by hydrogen puff and reached about $2 \times 10^{19}$ m$^{-3}$ when the puff was turned off at 1.33 s. The $\langle\beta_{dia}\rangle$ increased with $P_{abs}$ and $\bar{n}_e$, however, the increment seemed to be limited at 0.61 s although $\bar{n}_e$ continued to increase. The $\langle\beta_{dia}\rangle$ signal irregularly oscillated untill it started to decrease with the reduction of $P_{abs}$ at 1.86 s. The ratio of the net plasma current $I_p$ to $B_t$, $I_p/B_t$, stayed within 5 kA/T (Fig.1(c)) because the counter Ohkawa currents are cancelled out by the bootstrap currents flowing in the co-direction.

Figure 1(d) shows the temporal change of the poloidal component of the magnetic fluctuation with less than 50 kHz. A burst-like oscillation is observed up to 0.58 s in the low-density range with less than $0.7 \times 10^{19}$ m$^{-3}$, and the behavior is similar to the instabilities excited by high-energy ions, which was observed in previous experiments [7]. The amplitude of the fluctuation, which is normalized by $B_t$, abruptly increases at 0.78 s and was saturated immediately. The contour plot of the power spectrum density of this fluctuation is shown in Fig.1(h). A few peaks on the power spectrum are continuously observed during the discharge, and the strongest component with a frequency of about 1 kHz has $m/n$ = 2/1 structure and it rotates in the electron diamagnetic direction. The Figs.1(e-g) show the temporal changes of the amplitudes of the observed coherent components. Each amplitude corresponds to the root mean square of the coherent component extracted from

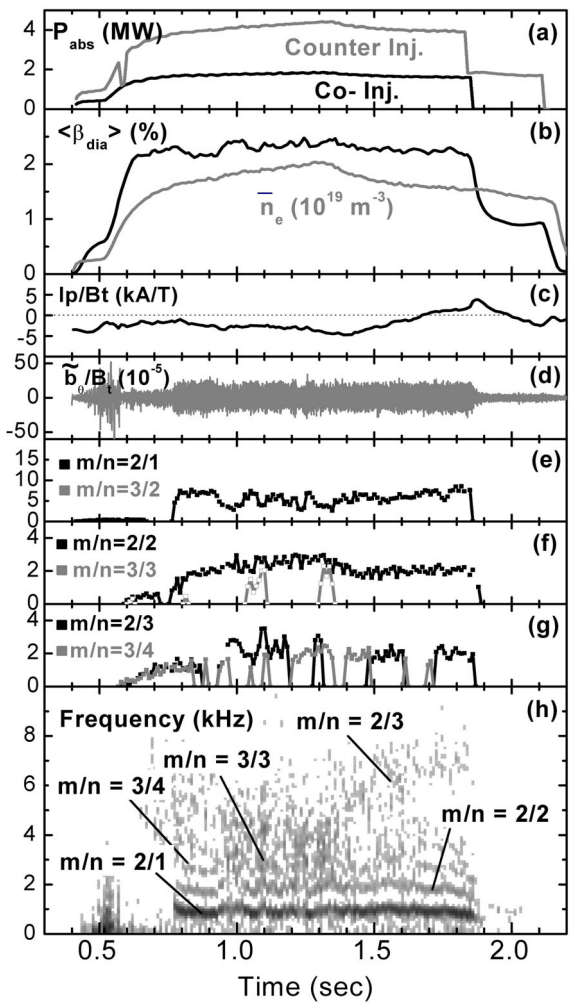


Fig. 1 Temporal changes of (a) absorbed heating power, (b) volume averaged beta value and line averaged electron density, (c) plasma current, (d) magnetic fluctuation, amplitudes of (e) $m/n = 2/1, 3/2$, (f) 2/2, 3/3, (g) 2/3, 3/4 and (h) power spectrum of magnetic fluctuation in the high-$\beta$ discharge with small plasma current.

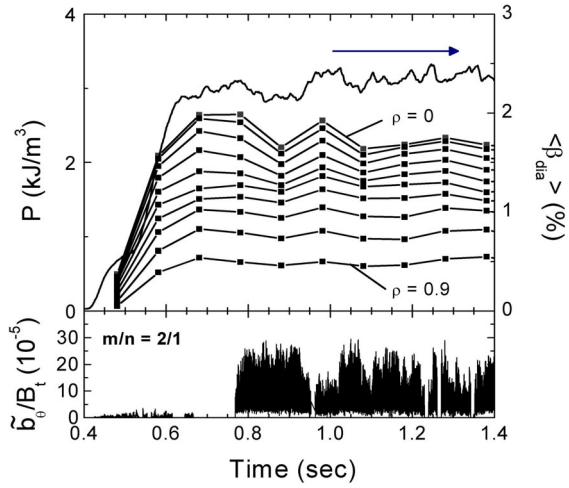


Fig. 2 Time evolutions of electron pressure at $\rho = 0 \sim 0.9$, volume averaged beta value and $m/n = 2/1$ mode in the Fig.1 discharge.

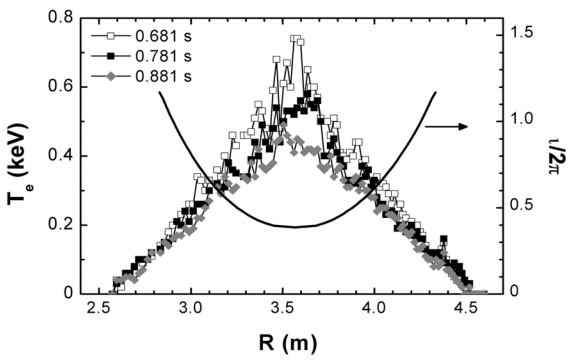


Fig. 3 Electron temperature profiles at 0.681, 0.781 and 0.881 s and rotational transform profile at 0.681 s.

the total fluctuation during 10 ms. The $m/n = 2/1$ mode abruptly grows at 0.76 s and then $\langle\beta_{\rm dia}\rangle$ decreases by about 10 %. The amplitude of the mode varies during the discharge, and the temporal change synchronizes the $\langle\beta_{\rm dia}\rangle$ signals. The $\iota/2\pi \geq 1$ resonant modes such as 2/2, 3/3, 3/4 and 2/3 start to grow at 0.59 s before $\langle\beta_{\rm dia}\rangle$ starts to be saturated at 0.61 s, and the onset times of these modes are earlier than that of the $m/n = 2/1$ mode. The temporal evolutions of amplitudes of MHD modes in the periphery such as the $m/n = 2/2$ mode depend on that of $\bar{n}_{\rm e}$ rather than $\langle\beta_{\rm dia}\rangle$. This result may be caused by the $\bar{n}_{\rm e}$ dependence of the formation of a peripheral pressure gradient and/or the dependence of the magnetic Reynolds number on the growth rate of resistive interchange mode [13].

Figure 2 shows the temporal changes of $\langle\beta_{\rm dia}\rangle$ and the local electron pressure $P_{\rm e}$ at each radial position from $\rho = 0$ to 0.9, and the amplitude of the $m/n = 2/1$ mode in the same discharge as in Fig.1. The pressure is defined as $P_{\rm e}(\rho) = 2n_{\rm e}(\rho)T_{\rm e}(\rho)$ and the time resolution is 100 ms. The pressures in the core region with $\rho \leq 0.4$ start to decrease just after the $m/n = 2/1$ mode is excited at 0.76 s. The decreases in $\langle\beta_{\rm dia}\rangle$ and $P_{\rm e}(0)$ at 0.875 s correspond to about 10 % and 20 %, respectively. The amplitude of the mode synchronizes with the core pressure as well as the $\langle\beta_{\rm dia}\rangle$ signal. The pressures in the region with $\rho \geq 0.5$ are almost constant even as the $m/n = 2/1$ mode is excited. They suggest that the oscillation of the $\langle\beta_{\rm dia}\rangle$ signal reflects the degradation and recovery of core electron stored energy caused by the activity of the mode.

The rotational transform profile at 0.681 s and $T_{\rm e}$ profiles at 0.681, 0.781 and 0.881 s are shown in Fig.3. The $\iota/2\pi = 1/2$ resonant surfaces are located at $R = 3.29$ and 3.88 m, which correspond to $\rho \sim 0.4$. The $T_{\rm e}(0)$ continues to decrease from about 0.75 keV at 0.681 s to 0.5 keV at 0.881 s with an increase in $n_{\rm e}$. A $T_{\rm e}$ profile with a discontinuous structure around the $\iota/2\pi = 1/2$ resonant surface

appears when the $m/n = 2/1$ mode has a large amplitude at 0.781 s. This structure disappears at 0.881 s with the reduction of the amplitude of the mode.

## 3.2 MHD activities in the large current plasmas

Figure 4 shows the discharge with different injection directions of neutral beams from the Fig.1 discharge. Two co- beams and one counter beam are injected into this discharge for a total $P_{abs}$ of about 3 MW at 1.7 s, as shown in Fig.4(a). The increase in $\langle\beta_{dia}\rangle$ is abruptly restricted when it reaches about 1.8 %, and $\langle\beta_{dia}\rangle$ starts to increase again at 1.16 s. Then, the increase in $\bar{n}_e$ is also enhanced, as shown in Fig.4(b). The value $I_p/B_t$, which consists of Ohkawa and bootstrap currents flowing in the same direction, increases with time, and approaches about 50 kA/T at 1.7 s (Fig.4(c)). The amplitude of the magnetic fluctuation abruptly increases at 0.8 s and then the increase in $\langle\beta_{dia}\rangle$ is restricted. The amplitude starts to decrease at 1.16 s. The $m/n = 2/1, 3/2, 2/2, 3/3, 3/4$ and 2/3 modes are observed in this discharge, and their characteristics are different from those observed in the Fig.1 discharge except for the $\iota/2\pi > 1$ resonant modes. The $m/n = 2/1$ mode is the most dominant one in all the frequency ranges with up to 50 kHz, and the amplitude of this mode increases at 0.8 s and approaches about $1.5 \times 10^{-4}$, which is about 1.8 times as large as that shown in Fig.1. This mode suddenly disappears at 1.2 s, and at the same time the $m/n = 3/2$ mode appears. Then the $I_p/B_t$ reaches about 30 kA/T and is expected to lead to the disappearance of the $\iota/2\pi = 1/2$ resonant surface. The $m/n = 3/2$ mode is not observed in Fig.1 discharge. The $m/n = 2/2$ and 3/3 modes start to grow at 0.68 s before the onset of the $m/n = 2/1$ mode. Although the amplitudes of these modes increase with $\bar{n}_e$ as well as in the Fig.1 case, they as well as $m/n = 2/1$ mode disappear at 1.2 s and appear occasionally after that. The amplitudes of $m/n = 2/3$ and 3/4 modes also increase with $n_e$.

The extended view of the time behavior of $\langle\beta_{dia}\rangle$ and the magnetic fluctuation from 0.6 to 1.4 s in the Fig.4 discharge are shown in Fig.5. When the $m/n = 2/1$ mode is destabilized from 0.8 to 1.2 s, $\langle\beta_{dia}\rangle$ is saturated around 1.8 % in spite of the increase in $\bar{n}_e$. The $\langle\beta_{dia}\rangle$ drastically increases with the decrease in the amplitude of the fluctuation from 1.18 s. However, $\langle\beta_{dia}\rangle$ continues to increase even after the stabilization of the mode at 1.2 s and approaches 2.4 % at 1.28 s. The profiles of $n_e, T_e$ and $P_e$ at 1.1, 1.2 and 1.3 s are shown in Fig.6. The $T_e$ in the core region with $\rho \leq 0.6$ at 1.2 s is higher than that at 1.1 s, and it corresponds to the decrease in the amplitude of the mode. The $T_e$ profile at 1.3 s is almost the same as that at 1.2 s. The $n_e$ profile has flattened at 1.1 s, and keeps the same form as it increases. The ramp-up rate of $\bar{n}_e$ from 1.2 s to 1.3 s is higher than that from 1.1 to 1.2 s, although the gas puff fueling is constant. As a result, the increase with $\langle\beta_{dia}\rangle$

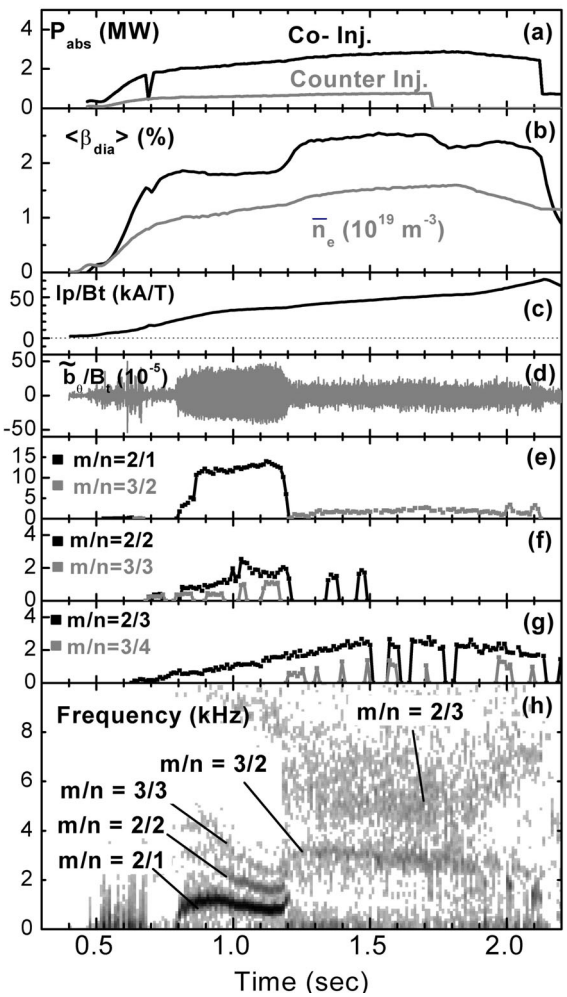


Fig. 4 Temporal changes of (a) absorbed heating power, (b) volume averaged beta value and line averaged electron density, (c) plasma current, (d) magnetic fluctuation, amplitudes of (e) $m/n = 2/1$, 3/2, (f) 2/2, 3/3, (g) 2/3, 3/4 and (h) power spectrum of magnetic fluctuation in the high-$\beta$ discharge with large plasma current.

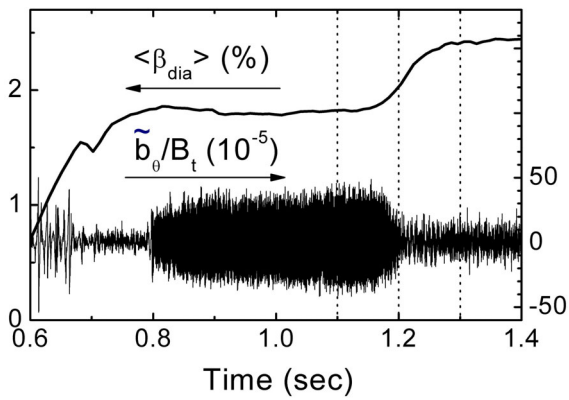


Fig. 5 Extended view of volume averaged beta value and magnetic fluctuation in the Fig.4 discharge.

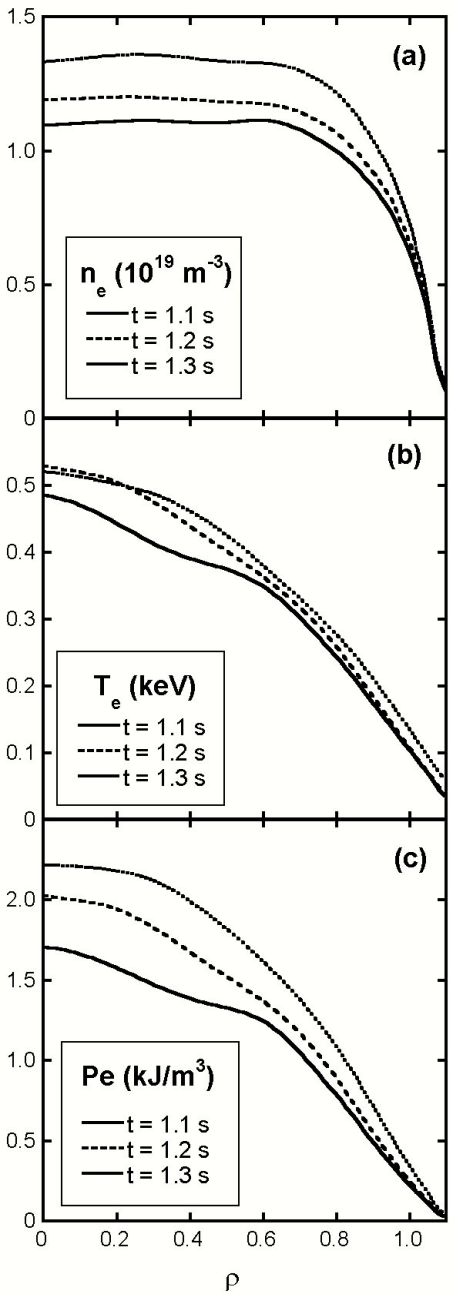


Fig. 6 (a) Electron density, (b) electron temperature and (c) electron pressure profiles at 1.1, 1.2 and 1.3 s in the Fig.4 discharge.

is caused by the increment of $n_e$ in the peripheral region in addition to the increase in $T_e$ in the core region.

## 3.3 Effects of MHD modes on the confinement

The changes of plasma parameters before and after the disappearance of the strong MHD modes as a function of $I_p/B_t$ are shown in Fig.7(a). The disappearance of the mode was observed in discharges with $I_p/B_t \geq 12$ kA/T in the obtained $I_p/B_t$ range with above zero. The $\langle\beta_{dia}\rangle$ is 1.8 ~ 2.0 % before this disappearance, and $\bar{n}_e$ decreases from 2 to $1 \times 10^{19}$ m$^{-3}$ when $I_p/B_t$ changes from 12 to 38 kA/T.

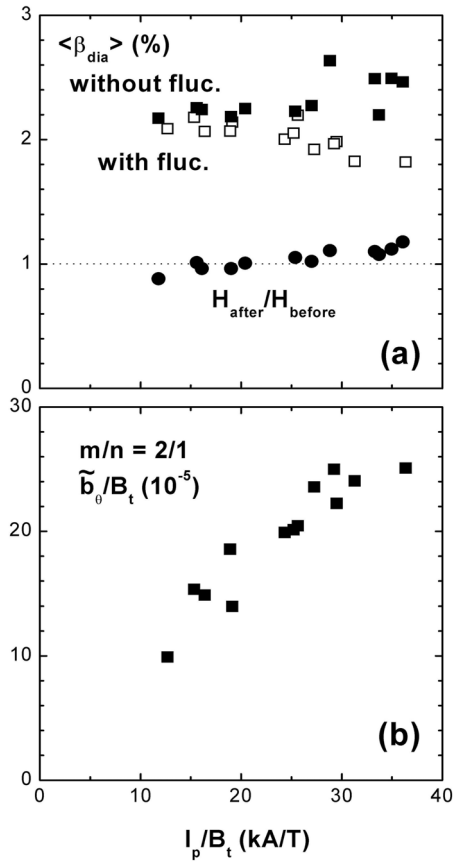


Fig. 7 Changes of (a) volume averaged beta value with/without the disappearance of the mode, the ratio of the $H$ factor after the event to that before the event and (b) amplitude of the $m/n = 2/1$ mode as a function of normalized plasma current.

The changes of $I_p/B_t$ may correspond to those of Ohkawa currents. While the increase in $\langle\beta_{dia}\rangle$ after the disappearance is less than 10 % when $I_p/B_t \leq 25$ kA/T, it increases in the range of $I_p/B_t \geq 25$ kA/T and approaches 38 % when $I_p/B_t = 38$ kA/T. The ratio of the improvement factor of the global energy confinement after an event to that before it, $H_{after}/H_{before}$, is about 1.0 at $I_p/B_t < 25$ kA/T and 1.0 ~ 1.2 at $I_p/B_t \geq 25$ kA/T. The improvement factor $H$ is defined as $\tau_E/\tau_{ISS95}$, where $\tau_E$ is the global energy confinement time in plasmas, estimated as $\tau_E = W_{dia}/P_{abs}$, and $\tau_{ISS95}$ is estimated by the so called International Stellarator Scaling 95 [14]. One of the reasons for this difference is the broadening of the deposition profile of neutral beams. Since the direction of neutral beams is optimized to magnetic configurations with $R_{ax} \geq 3.6$ m, the peak of the deposition profile shifts to the outward direction with an increase in $n_e$. The ratio of the $\tau_E/\tau_{ISS95}$ before and after the disappearance increases when $I_p/B_t$ exceeds 25 kA/T and reaches 1.2 at $I_p/B_t = 38$ kA/T. The change of the amplitude of the $m/n = 2/1$ mode as a function of $I_p/B_t$ is shown in Fig.7(b). The amplitude is about $10^{-4}$ when $I_p/B_t$ is 12 kA/T and is almost the same level as that in the

currentless plasmas as shown in Fig.1 (a). The amplitude increases with $I_p/B_t$ and approaches $2.5 \times 10^4$ at $I_p/B_t$ = 38 kA/T. The gradual increase in the amplitude is qualitatively consistent with the degree of the recovery of $\langle\beta_{dia}\rangle$ in the range with $I_p/B_t < 25$ kA/T. However, the tendency is quite inconsistent with the abrupt increase in $\langle\beta_{dia}\rangle$ in the $I_p/B_t$ range with > 25 kA/T, and the $\iota/2\pi = 1$ resonant modes have not been observed in this region. The sufficient increment of $\langle\beta_{dia}\rangle$ and the improvement of the confinement may be caused by the stabilization of the $\iota/2\pi = 1$ resonant modes as described in Sec. 3.2.

### 3.4 Appearances and amplitudes of MHD modes

Figure 8 shows the appearances and the amplitudes of observed MHD modes in the $I_p/B_t$ and $\langle\beta_{dia}\rangle$ diagram. Twenty discharges in the configuration with $R_{ax} = 3.5$ m and $B_t = 0.5$ T are applied and their histories untill NBIs were turned off are plotted. The dotted and solid lines are in the ramp-up phase of the stored energy and in the quasi-steady state, respectively. The color of the closed circle indicates the relative amplitude of the MHD mode, which is normalized by the strongest amplitude in all the observed modes. As shown in this figure, the $m/n = 2/1$ mode has the strongest amplitude, especially in the plasmas with large $I_p/B_t$. The amplitude is dependent on $I_p/B_t$ and $\langle\beta_{dia}\rangle$. The increase in $I_p/B_t$ enhances the mode, which is caused by the reduction of the magnetic shear. The amplitude decreases with an increase in $\langle\beta_{dia}\rangle$ as shown in the low $I_p/B_t$ regime with less than 10 kA/T. The reason may be that the destabilization effect due to the magnetic hill is weakened by a Shafranov shift. The complete disappearance of the mode has been found in high $I_p/B_t$ and high $\langle\beta_{dia}\rangle$, which is due to the disappearance of the resonant surface, and large $I_p/B_t$ seems to realize higher $\langle\beta_{dia}\rangle$ than the low $I_p/B_t$ case.

The $m/n = 3/2$ mode has hardly been observed in the discharges with $I_p/B_t < 10$ kA/T, and like the $m/n = 2/1$ mode case, its amplitude of the mode increases with $I_p/B_t$. Its beta dependence is not clear. The disappearance of the mode was not found in the present $I_p/B_t$ range. An interpretation of this tendency is presented in Sec. 4.

The $m/n = 2/2$ mode has been observed in the $I_p/B_t$ range with less than 25 kA/T and the amplitude increases with $\langle\beta_{dia}\rangle$. However, the mode intermittently appears or disappears when $I_p/B_t$ exceeds a certain value as shown in the Fig.4 discharge. Also, the amplitude seems to depend on the absolute value of $I_p/B_t$. In the $I_p/B_t$ region with less than 10 kA/T, the amplitude looks like to depend on $\langle\beta_{dia}\rangle$. The $m/n = 2/3$ mode has been observed in all the present ranges. The amplitude strongly depends on $\langle\beta_{dia}\rangle$, and the $I_p/B_t$ dependence is relatively weak.

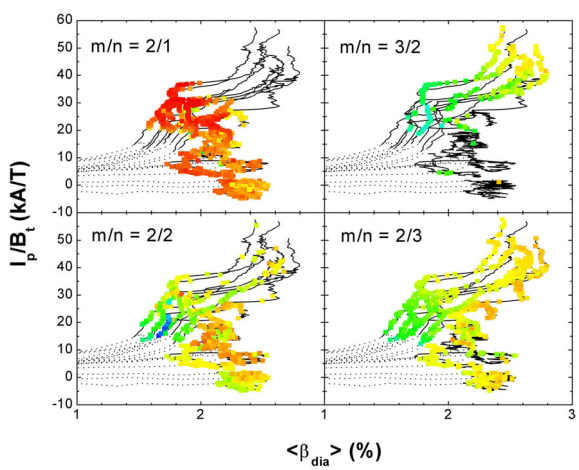


Fig. 8 Appearances and amplitudes of $m/n = 2/1, 3/2, 2/2$ and 2/3 modes in the $I_p/B_t$ and $\beta_{dia}$ diagram.

## 4. Discussion and Summary

According to linear MHD theory, the destabilization of the interchange mode driven by the pressure gradients as the free energy source strongly depends on magnetic configurations formed by external coils and modified by net plasma currents. The validity of this theory has been investigated in various experiments. Also, the magnetic Reynolds number, $S$, is the parameter able to influence the growth rate of the mode. The increment of $S$ decreases the growth rate of the resistive mode [13], and a plasma with $S = \infty$ approaches the ideal condition. The $S$ in the core region of the LHD plasma is typically $10^7 - 10^8$. Such plasma is suitable for comparison with the linear growth rate of the ideal mode [13]. The amplitudes of the modes observed in LHD are much smaller than those in CHS experiments with $S = 10^4 - 10^5$ [4]. These results can be interpreted by the reduction of the growth rate on the assumption that it is related to the extension of the radial structure of the modes.

Experiments in the unstable configuration of the ideal MHD mode are valid for investigating the effect of the ideal mode on plasma confinement. The LHD has a wide flexibility of configuration through control of $R_{ax}$, and the $R_{ax} = 3.5$ m configuration selected here is the most unstable one with a highly magnetic hill in the present operation regime. In the currentless plasmas, the Mercier criterion, $D_I$, at the $\iota/2\pi = 1/2$ resonant surface transiently approaches about 1.5 before profile deformation due to $m/n = 2/1$ mode activity, which corresponds to about three times as high as the case of $R_{ax} = 3.6$ m configuration with the same $\langle\beta_{dia}\rangle$. The amplitude of the observed mode in the $R_{ax} = 3.5$ m case is several times as high as that in the $R_{ax} = 3.6$ m case, and the mode leads to the 10 % degradation of the confinement even in currentless plasmas as shown in Fig.1. The mode is enhanced further when the plasma current is increased, and it restricts the increment of the $\langle\beta_{dia}\rangle$ more and more. While the $D_I$ at the $\iota/2\pi = 2/3$ surface, which is located just outside $\iota/2\pi = 1/2$ surface, is about 0.3 in plasmas with

$\langle\beta_{\rm dia}\rangle = 2\,\%$ and $I_{\rm p}/B_{\rm t} < 10\,$kA/T, the $m/n = 3/2$ mode was not observed or was intermittently observed during the discharge. Like the $m/n = 2/1$ mode, this mode is enhanced with an increase in the plasma current. These results are similar to the results of the CHS experiments [8], indicating the significance of the magnetic shear. The plasma current can make various rotational transform profiles such as radial extension of the resonance and/or the double resonance by a variation of its profile, and the reduction of the magnetic shear impacts the degree of the extension of the radial structure of the mode.

The disappearance of the $m/n = 2/1$ mode may correspond to exclusion of the resonant surface due to a positive plasma current. It happens in a wide range of plasma currents as shown in Fig.7, and may be caused by the change of the current profile. If the current profile changes from flattened one to a peak as a function of $n_{\rm e}$, the $\iota/2\pi = 1/2$ surface can disappear in spite of a different net current. The change of current profile as a function of $n_{\rm e}$ mainly occurs in Ohkawa currents rather than bootstrap currents. The recently developed MSE measurements are expected to clarify the temporal change of the plasma current profile.

The improvement of plasma confinement after the disappearance of MHD activity becomes remarkable when the plasma current exceeds a certain value. One possible explanation for this phenomena is that the confinement in the peripheral region is improved by the stabilization of the $\iota/2\pi = 1$ resonant modes due to the increase in the plasma current. In discharges with a small plasma current, the $\iota/2\pi = 1$ resonant modes are observed just after the $m/n = 2/1$ mode disappears. Then $\langle\beta_{\rm dia}\rangle$ changes by less than 10 %, which is caused by the increase in the $T_{\rm e}$ in the core region. A similar phenomenon was observed in the high-$\beta$ experiment in the $R_{\rm ax} = 3.6\,$m configuration [4]. The $\iota/2\pi = 1$ resonant modes disappear with the $m/n = 2/1$ mode in the discharge with the large plasma current as shown in Fig.4. Then the pressure in the peripheral region increases after the increase in the core pressure. The stabilization of the $\iota/2\pi = 1$ resonant modes may lead to improvement of the confinement in the peripheral region. Peripheral MHD activities are a major subject in high-$\beta$ plasmas, and the effects on the plasma confinements have been investigated [15]. The mechanism of the stabilization is not clear because the plasma current is too small to eliminate the $\iota/2\pi = 1$ resonant surface. Although it is theoretically predicted that the increase in pressure gradient destabilizes the pressure driven mode, the $\iota/2\pi = 1$ resonant modes disappear in spite of the increase in pressure gradient as shown in Fig.6.

In summary, the effects of resonant magnetic fluctuations on plasma confinement have been investigated in current-carrying high-$\beta$ plasmas with finite plasma currents. The $m/n$= 2/1 mode excited in the core region was dominantly observed in the unstable configuration, as predicted by linear theory on ideal instability, and the plasma current decreasing magnetic shear enhanced the mode activity. The disappearance of the $m/n = 2/1$ mode was observed when the plasma current increased. The plasma confinement and the beta value increase by less than 10 % with the recovery of core pressure. When the plasma current exceeded a certain value, the plasma confinement was improved by 20 % with the reduction of the amplitudes of the modes in the peripheral region in addition to the disappearance of the $m/n = 2/1$ mode. Then the beta value increased by 38 %. MHD activities lead to no disruption even in such an *unstable* configuration, and the moderate plasma current mitigated the effect of MHD activity on the plasma confinement.

## Acknowledgments

The authors acknowledge the continuous effort of all members of the device engineering group. This work is supported by NIFS under Contract No.ULHH517.

[1] Y.Q. Liu *et al.*, Phys.Plasmas **7**, 3681 (2000).
[2] A. Isayama *et al.*, Nucl. Fusion **43**, 1272 (2003).
[3] S. Sakakibara *et al.*, Nucl. Fusion **41**, 1177 (2001).
[4] S. Ohdachi *et al.*, *Proc. 13th Int. Stellarator Workshop*, Canberra, Australia, February 25–March 1, 2002.
[5] S. Sakakibara *et al.*, Plasma Phys. Control Fusion **44**, A217 (2002).
[6] K.Y. Watanabe *et al.*, Fusion Sci. Tech. **46**, 24 (2004).
[7] K. Toi *et al.*, Nucl. Fusion **44**, 217 (2004).
[8] S. Sakakibara *et al.*, J. Journal Appl. Phys. **34**, pt2, 2B, 252 (1995).
[9] K. Toi *et al*, Plasma Phys. Control. Fusion **38**, 1289 (1996).
[10] K.Y. Watanabe *et al.*, Journal of Plasma and Fusion Research SERIES **5**, 124 (2003).
[11] O. Motojima *et al.*, Nucl. Fusion **43**, 1674 (2003).
[12] S.P. Hirshman and W.I. van RIJP. Merkel, Comput. Phys. Commun. **43**, 143 (1986).
[13] K. Ichiguchi *et al.*, Nucl. Fusion **29**, 2093 (1989).
[14] U. Stroth *et al.*, Nucl. Fusion **36**, 1063 (1996).
[15] K.Y. Watanabe *et al.*, Nucl. Fusion **45**, 1247 (2005).